J|A|C|S ARTICLES

Published on Web 03/02/2009

Pressure-Induced Cooperative Bond Rearrangement in a Zinc Imidazolate Framework: A High-Pressure Single-Crystal X-Ray Diffraction Study

Elinor C. Spencer,*,† Ross J. Angel,† Nancy L. Ross,† Brian E. Hanson,† and Judith A. K. Howard‡

Department of Geosciences and Department of Chemistry, Virginia Tech University, Blacksburg, Virginia 24061, and Department of Chemistry, Durham University, South Road, Durham DH1 3LE, U.K.

Received October 30, 2008; E-mail: espence@vt.edu

Abstract: The pressure-dependent structural evolution of a neutral zinc-imidazolate framework $[Zn_2(C_3H_3N_2)_4]_n$ (ZnIm) has been investigated. The as-synthesized three-dimensional ZnIm network (α-phase) crystallizes in the tetragonal space group $I4_1cd$ ($a = 23.5028(4)$ Å, $c = 12.4607(3)$ Å). The ZnIm crystal undergoes a phase transition to a previously unknown β-phase within the 0.543(5)−0.847(5) GPa pressure range. The tetragonal crystal system is conserved during this transformation, and the β-phase space group is $I4_1$ ($a = 22.7482(3)$ Å, $c = 13.0168(3)$ Å). The physical mechanism by which the transition occurs involves a complex cooperative bond rearrangement process. The room-temperature bulk modulus for ZnIm is estimated to be ~14 GPa. This study represents the first example of a high-pressure single-crystal X-ray diffraction analysis of a metal−organic framework.

Introduction

The synthesis of metal−organic hybrid materials has been at the forefront of chemical research for some years, and a plethora of published examples of such complexes exists.[1] However, the development of this class of materials for practical applications has only recently begun to receive significant attention. Some of the most promising areas for which hybrid materials are potentially useful candidates include gas-separation, heterogeneous catalysis, and gas-storage,[2−6] and all of these applications involve placing the metal−organic framework (MOF) under pressure. To date, the maximum pressure to which MOFs are subjected to, and as such are expect to endure without disintegration or phase conversion, is ~100 bar (0.01 GPa). That said, as research in this field progresses and MOFs are tailored to satisfy a wider range of functions, one may expect an increase in the pressure range over which structural stability is desirable.

There is clearly a need to understand the structural response of MOFs to applied pressure. Nevertheless, hitherto there are very few published investigations dedicated to determining the behavior of porous hybrid materials under pressure. The few structural reports that do exist are primarily concerned with the deformation of the hybrid networks in response to the inclusion of guest molecules (either gases or solvents) within the network cavities, rather than consideration of the pressure-induced evolution of the hybrid structure itself in the absence of guest species.[7−11] It is this information deficit that provided the impetus for the high-pressure single-crystal X-ray diffraction (HP-XRD) study reported herein.

We chose to investigate the pressure-induced structural evolution of the zinc-imidazolate framework $[Zn_2(C_3H_3N_2)_4]_n$ (ZnIm). Our rationale for studying this particular MOF is threefold: (i) Good diffraction-quality ZnIm crystals are easy to prepare via a simple solvothermal synthesis method and are stable under ambient laboratory conditions for at least 1 year. (ii) The ZnIm crystals belong to the highly symmetric tetragonal crystal system. This reduces the volume of reciprocal space that must be measured during a diffraction experiment to enable the refinement of the crystal structure. This is particularly advantageous for HP-XRD measurements, as the volume of reciprocal space that can be accessed is limited by the geometry of the experimental apparatus employed. (iii) The neutral ZnIm framework is known to be well ordered in the crystalline state. Additionally, the cavities of the framework are devoid of counterions and solvent molecules. Both of these factors

† Virginia Tech University.
‡ Durham University.

(1) Robin, A. Y.; Fromm, K. M. *Coord. Chem. Rev.* **2006)** , *250*, 2127.
(2) Férey, G. *Chem. Soc. Rev* **2008)** , *37*, 191.
(3) Mueller, U.; Schubert, M.; Teich, F.; Puetter, H.; Schierle-Arndt, K.; Pastré, J. *J. Mater. Chem* **2006**, *16*, 626.
(4) Zhou, W.; Wu, H.; Hartman, M. R.; Yildirim, T. *J. Phys. Chem. C* **2007**, *111*, 16131.
(5) Kitagawa, S.; Kitaura, R.; Noro, S. *Angew. Chem. Int. Ed.* **2004**, *43*, 2334.
(6) Champness, N. R. *Dalton Trans.* **2006**, 877.
(7) Fletcher, A. J.; Cussen, E. J.; Prior, T. J.; Rosseinsky, M. J.; Kepert, C. J.; Thomas, K. M. *J. Am. Chem. Soc.* **2001**, *123*, 10001.
(8) Kachi-Terajima, C.; Akatsuka, T.; Kohbara, M.; Takamizawa, S. *Chem. Asian J.* **2007**, *2*, 40.
(9) Zhao, Y.; Xu, H.; Daemen, L. L.; Lokshin, K.; Tait, K. T.; Mao, W. L.; Luo, J.; Currier, R. P.; Hickmott, D. D. *Proc. Nat. Acad. Sci.* **2007**, *104*, 5727.
(10) Kitaura, R.; Kitagawa, S.; Kubota, Y.; Kobayashi, T. C.; Kindo, K.; Mita, Y.; Matso, A.; Kobayashi, M.; Chang, H.-C.; Ozawa, T. C.; Suzuki, M.; Sakata, M.; Takata, M. *Science* **2002**, *298*, 2358.
(11) Takamizawa, S.; Nakata, E.; Saito, T.; Kojima, K. *CrystEngComm* **2003**, *5*, 411.

10.1021/ja808531m CCC: $40.75

Table 1. Crystallographic Data Collection and Refinement Details

	pre-DAC (α-phase)	P0 (α-phase)	P1 (α-phase)	P2 (α-phase)	P3 (α-phase)	post-DAC (β-phase)[a]
pressure (GPa)	ambient	0.000100(1)	0.092(5)	0.295(6)	0.543(5)	ambient
T (K)	298	298	298	298	298	298
cryst no.	1	1	1	1	1	2
cryst size (μm^3)	420 × 96 × 96	420 × 96 × 96	420 × 96 × 96	420 × 96 × 96	420 × 96 × 96	185 × 134 × 106
chemical formula	$Zn_2C_{12}H_{12}N_8$	$Zn_2C_{12}H_{12}N_8$	$Zn_2C_{12}H_{12}N_8$	$Zn_2C_{12}H_{12}N_8$	$Zn_2C_{12}H_{12}N_8$	$Zn_2C_{12}H_{12}N_8$
cryst syst	tetragonal	tetragonal	tetragonal	tetragonal	tetragonal	tetragonal
space group	$I4_1cd$	$I4_1cd$	$I4_1cd$	$I4_1cd$	$I4_1cd$	$I4_1$
Z	16	16	16	16	16	16
a (Å)	23.5028(4)	23.4856(6)	23.3569(5)	23.2297(4)	23.0474(6)	22.7482(3)
c (Å)	12.4607(3)	12.4521(7)	12.4441(6)	12.4296(5)	12.4020(7)	13.0168(3)
V (Å^3)	6883.1(2)	6868.2(5)	6788.8(4)	6707.2(3)	6587.7(4)	6735.9(2)
ρ_{calcd} (g cm^{-3})	1.540	1.544	1.562	1.581	1.609	1.574
μ (Mo K$_\alpha$) (mm^{-1})	2.79	2.80	2.83	2.85	2.92	2.86
collected reflns	31 180	49 902	51 336	51 091	50 038	26 566
unique reflns	3028	2923	3013	3018	2958	5974
R (int)	0.0443	1.021	0.986	1.015	1.005	0.0665
no. of params	199	77	77	77	77	400
no. of restraints	1	37	37	37	37	1
GOF	0.884	0.912	0.835	0.851	0.894	0.900
$R1$ [$I > 2\sigma(I)$]	0.0276	0.0773	0.0596	0.0639	0.0829	0.0382
wR2 [$I > 2\sigma(I)$]	0.0401	0.0970	0.0630	0.0491	0.0894	0.0516

[a] Data for the second crystal rather than the first are reported, as this crystal broke into larger fragments that provided better quality XRD data.

decrease the number of potential complications that may arise during the refinement of the ZnIm structures derived from HP-XRD data.

Experimental Section

Synthesis. $Zn(NO_3)_3 \cdot 6H_2O$ (0.0298 g, 0.1 mmol), imidazole (0.136 g, 2.0 mmol), DMF (4 mL), and butanol (2 mL) were placed in a 25 mL Teflon-lined steel bomb. The bomb was placed in a preheated oven at 150 K and heated for 5 days. After being cooled, the contents of the steel bomb were filtered and washed twice with ethanol. Colorless crystals of ZnIm were found embedded within an unidentified white powder and were removed by hand.

Crystallography. Prior to HP-XRD analysis, data were collected with the ZnIm single crystal under ambient conditions on an Oxford Diffraction Gemini diffractometer equipped with a CCD detector and operating with monochromated Mo Kα radiation ($\lambda = 0.71073$ Å). The data were processed with standard Oxford Diffraction software.[12] Structural solution was via direct methods, and refinement was on F^2 using full-matrix least-squares refinement techniques. All non-hydrogen atoms were refined ansiotropically. Hydrogen atoms were included in the model at calculated positions and refined with a riding model with their U_{iso} value set to $1.2U_{eq}$ of the parent atom.

For HP-XRD data collections, the ZnIm crystal was placed in a standard ETH diamond anvil cell (DAC).[13] To enable pressure calibration, a quartz crystal was positioned alongside the ZnIm crystal. The pressure within the cell was calculated from measurements of the quartz unit cell volume.[14] The gasket cavity was filled with anhydrous 2-propanol that acted as a nonpenetrating pressure medium and is known to remain hydrostatic up to 4.2 GPa.[15] HP-XRD data were collected on an Oxford Diffraction Xcalibur instrument with monochromated Mo Kα radiation ($\lambda = 0.71073$ Å). The diffractometer was fitted with a CCD detector. Data were integrated using standard Oxford Diffraction software.[12] Absorption corrections were applied with the ABSORB program, and the data corrected for DAC dips and other anomalies by AVERAGE.[16a,b] Structural refinements were performed on F^2 using full-matrix least-squares refinement techniques. All atoms were refined isotropically due to the limited data available. The imidazole rings were constrained to chemically reasonable geometries. Hydrogen atoms were included in the refinement model at calculated positions and refined with a their U_{iso} values set to $1.2U_{eq}$ of the parent atom.

Precise unit cell parameters (Table 1) were determined on a Huber diffractometer with an Eulerian cradle[14] equipped with a point detector. The method used was based on eight-position centring of 28−30 reflections, $9° < 2\theta < 21°$, following procedures of Angel et al., and Ralph and Finger.[14,17a,b]

After all HP-XRD data collections were complete, the ZnIm crystal was recovered from the DAC. The crystal had fragmented

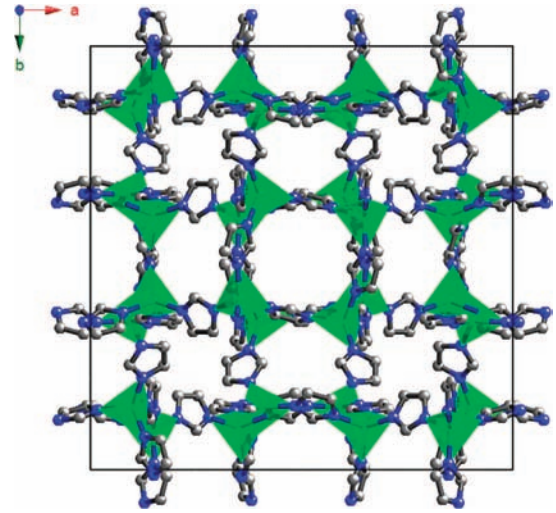

Figure 1. α-Phase of ZnIm framework as view down the crystallographic c axis (Zn, green; N, blue; C, gray). Hydrogen atoms have been omitted for clarity.

(12) Data collection and processing software: CCD and RED (versions 171.32), Oxford Diffraction Ltd., Abingdon, England (2008). Structure solution and refinement software: WinGX (v1.70.01). Farrugia, L. J. *J. Appl. Crystallogr.* **1999**, *32*, 837.

(13) Miletich, R.; Allan, D. R.; Kuhs, W. F. *High-Temperature and High-Pressure Crystal Chemistry*; Hazen, R. M., Downs, R. T., Eds.; Mineralogical Society of America: Washington, DC, **2000**; Vol. 41, pp 445−519.

(14) Angel, R. J.; Allan, D. R.; Miletich, R.; Finger, L. W. *J. Appl. Crystallogr.* **1997**, *30*, 461.

(15) Angel, R. J.; Bujak, M.; Zhao, J.; Gatta, G. D.; D Jacobsen, S. *J. Appl. Crystallogr.* **2007**, *40*, 26.

(16) (a) ABSORB 61. Angel, R. J. J. Appl. Crystallogr. *37*, 486 (**2004**). (b) AVERAGE 2.21. Angel, R. J. 2005.

(17) (a) King Jr, H.; Finger, L. W. *J. Appl. Crystallogr.* **1979**, *12*, 374. (b) Ralph, R. L.; Finger, L. W. *J. Appl. Crystallogr.* **1982**, *15*, 537.

Table 2. Selected Bond Lengths (Å) and Angles (deg) for the ZnIm α-Phase[a]

bond length/angle	pre-DAC	P0	P1	P2	P3
Zn1−N1	1.975(4)	1.94(2)	1.95(2)	1.90(2)	1.91(2)
Zn1−N3	1.993(4)	1.96(2)	1.95(2)	1.93(2)	1.87(2)
Zn1−N5	1.977(4)	1.94(2)	1.93(2)	1.90(2)	1.96(2)
Zn1−N7	1.979(4)	1.97(2)	2.02(2)	1.99(2)	1.95(2)
Zn2−N2	1.991(4)	2.00(2)	1.95(2)	1.94(2)	2.01(2)
Zn2−N4	1.987(4)	2.04(2)	2.01(2)	2.03(2)	2.05(3)
Zn2−N6	2.005(4)	2.06(2)	2.04(2)	2.05(2)	1.93(3)
Zn2−N8	1.975(3)	2.00(2)	1.95(2)	1.93(2)	1.94(2)
N1−Zn1−N3	111.1(2)	110.7(9)	108.4(9)	109(1)	111(1)
N1−Zn1−N5	107.8(2)	110.1(9)	109(1)	109(2)	108(1)
N1−Zn1−N7	113.9(2)	112.2(9)	114.0(9)	114.7(9)	114(1)
N3−Zn1−N5	106.4(2)	107.3(8)	109(1)	111(1)	111(1)
N3−Zn1−N7	105.9(2)	103.7(8)	104(1)	102(1)	102(1)
N5−Zn1−N7	111.6(2)	113(1)	111.8(9)	110.2(9)	110(1)
N2−Zn2−N4	107.9(2)	110.9(9)	109(1)	109(1)	109(1)
N2−Zn2−N6	110.1(2)	107.5(9)	108.2(9)	109.4(9)	109(1)
N2−Zn2−N8	111.9(2)	111.8(8)	111.5(9)	113.2(9)	111(1)
N4−Zn2−N6	104.3(2)	104.1(9)	104(1)	103(1)	101(1)
N4−Zn2−N8	116.3(2)	116.9(8)	118(1)	118(1)	119(1)
N6−Zn2−N8	105.0(2)	104.7(9)	104(1)	104(1)	107(1)

[a] For atom labelling scheme see Figure S1 (Supporting Information).

as a result of a pressure-induced phase transition (see Results and Discussion section). Data were collected, under ambient conditions, with one of the crystal fragments that appeared to be single when viewed under a microscope with crossed polarisers. Data were collected and processed using the same procedure detailed above for the pre-DAC data collection. The crystal was found to be a 4-fold merohedral twin. The twin operators were determined to be a 2-fold axis along the (110) direction and an inversion center. Once the zinc atoms had been located from difference Fourier maps, the twin laws were implemented, and the refinement proceeded without further complications.

To ensure the reproducibility of these results, a second ZnIm crystal was placed in the DAC and the pressure slowly increased to ~0.815 GPa. The crystal cracked in the 0.6−0.8 GPa pressure range; this behavior was also observed for the first crystal within the same pressure range. The crystal fragments were recovered, and XRD analysis under ambient conditions confirmed that this second crystal had undergone a phase transition in an analogous manner to the first. Additional crystallographic information for all data collections is given in Table 1.

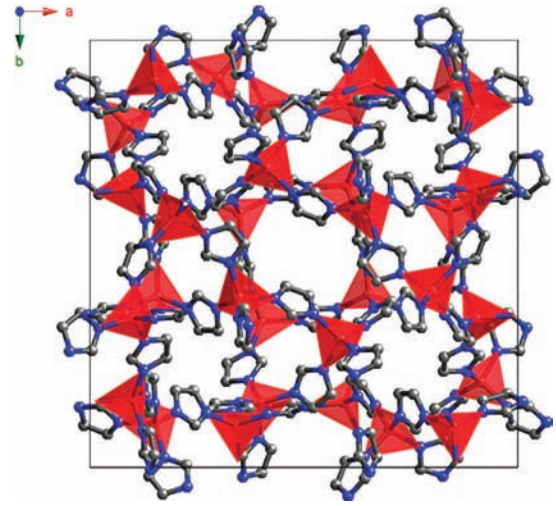

Figure 3. β-Phase of ZnIm framework as viewed down the crystallographic *c* axis (Zn, red; N, blue; C, gray). Hydrogen atoms have been omitted for clarity.

Results and Discussion

Von Lenhert et al. reported the crystal structure of α-phase ZnIm in 1980;[18] the macromolecular ZnIm complex crystallizes in the tetragonal space group $I4_1cd$, and is a three-dimensional MOF. The nodal points of the network comprise discrete Zn^{2+} cations, rather than multifaceted metal clusters, that are bridged by imidazolate anions to afford a neutral uninodal 4-connected net (Figure 1).[19] All the Zn^{2+} ions reside in distorted tetrahedral coordination environments, with the N−Zn−N angles varying widely within the range 104.3(2)−116.3(2)° (Table 2). The distance between Zn^{2+} ions bridged by an imidazolate anion is ~6.0 Å, and the structure contains solvent accessible voids of ~76 Å^3.[3,20] However, the neutrality of the framework negates the need for counterions, and consequently the cavities are devoid of any molecular species.

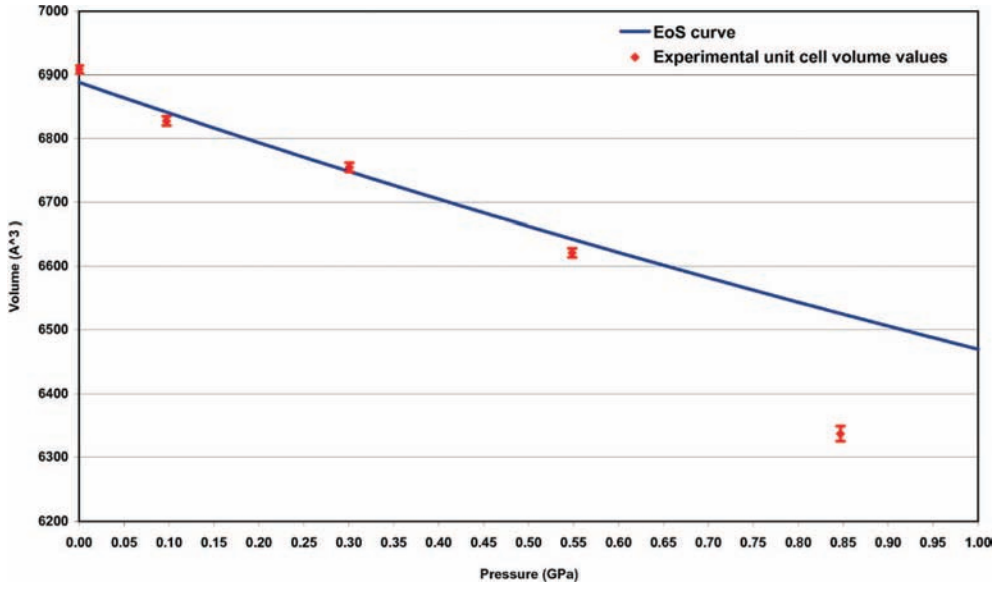

Figure 2. Plot showing the evolution of the ZnIm unit cell volume with pressure. The experimental unit cell volumes are calculated from the HP-XRD data recorded with a CCD detector. The line is an EoS curve with a bulk modulus of $K_0 = 14$ GPa, and $K' = 4$.

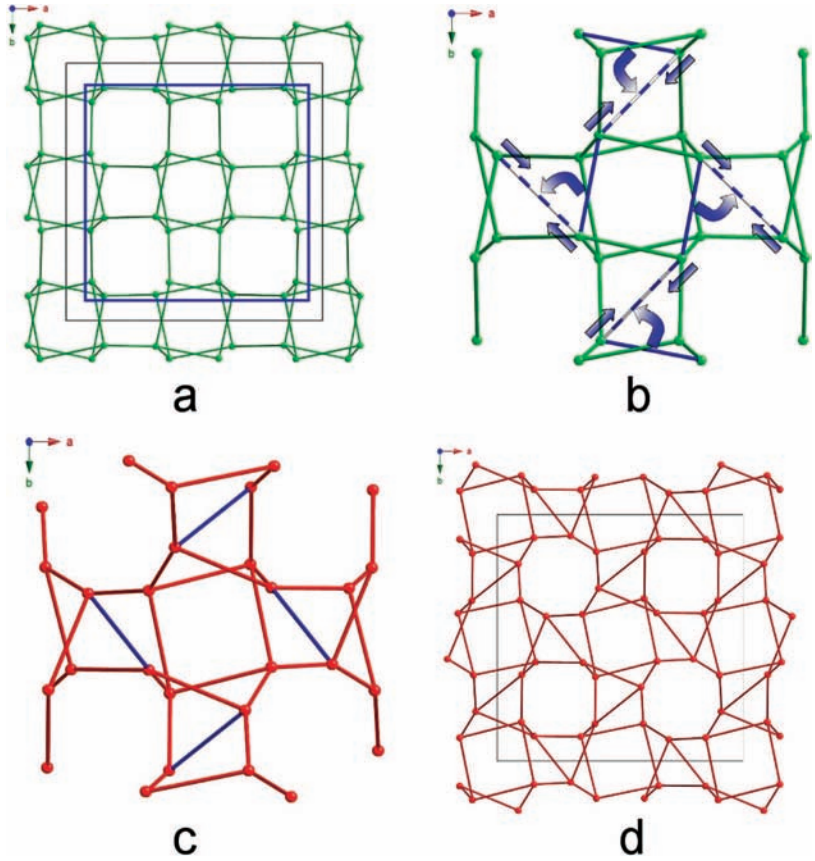

Figure 4. (a) Ball-and-stick representation of the ZnIm α-phase; the Zn^{2+} cations are shown as balls and the imidazolate ions as sticks. (b) A close-up of the structure within the blue square displayed in Figure 4a. This diagram shows the cooperative bond rearrangement that occurs during the α→β phase transition. The solid blue lines are the links that are broken during the transition, and the blue and white stripped lines show the locations where the imidazolate links are reformed. (c) The ZnIm β-phase. The blue lines show the new positions for the imidazolate links that moved during the transition. (d) Ball-and-stick representation of the ZnIm β-phase.

Figure 2 is a plot showing the evolution of the ZnIm unit cell volume as a function of pressure. Due to the limited pressure range over which HP-XRD data were collected, it is not possible to fit an equation of state (EoS) to the data to enable the bulk modulus of ZnIm to be determined accurately. An approximation with a second-order Birch−Murnagan EoS shown in Figure 2, and this indicates that the data are consistent with a room pressure bulk modulus (K_0) of about 14 GPa for ZnIm.[21] For comparison, molecular solids typically have K_0 values less than 30 GPa, and zeolites have K_0 values in the 19−59 GPa range.[22−24] There are very few K_0 values for molecular solids reported in the literature, nonetheless a few examples can be found, and these include $K_0 = 29.1(4)$ GPa for L-cystine,[25] $K_0 = 17.6(4)$ GPa for 1,1-diamino-2,2-dinitroethylene,[26,27] and 6.6 GPa for $Ru_3(CO)_{12}$.[28] Dinnebier et al. reported K_0 values within the range of 4.9(3)−18(2) GPa for polymeric metallocenes.[29]

Figure 2 shows that the experimental data point at ∼0.85 GPa deviates significantly from the EoS plot that approximates the compression of the unit cell at pressures below ∼0.54 GPa. This behavior is indicative of the ZnIm crystal having undergone a phase transition between 0.54−0.85 GPa. As a consequence of the phase transition the ZnIm crystal fragments, and HP-XRD data for the β-phase are of an insufficient quality, due to peak splitting and reduced resolution, to enable structural solution. Therefore, the structure of the β-phase (Figure 3) was determined from single-crystal XRD data recorded under ambient conditions with a fragment of the crystal that was recovered from the DAC (see Experimental Section for further details).

There is a reduction in the space group symmetry as the crystal converts from $I4_1cd$ (α-phase) to the subgroup $I4_1$ (β-phase). Figure 4 provides a schematic of the structural alteration that occurs during the phase change, the mechanism for which involves cooperative bond rearrangement. If one regards the principle motif of the ZnIm structure as puckered squares with Zn^{2+} ions locates at the vertices and imidazolate anions along the edges, then the α-phase can be regarded as infinite columns of stacked squares running parallel to the *c*- axis, with the squares within these columns related by the 4_1 screw axes. Adjacent squares are rotated with respect to each other (Figure 4a), and are bridged at diagonal corners by imidazolate anions. Neighboring columns are connected in the [1 0 0] and [0 1 0] directions by imidazolate ligands. During the phase transition alternate squares within the columns undergo the bond rearrangement shown in Figure 4b resulting in the formation of the denser β-phase (Figure 4c and d). The remaining 50% of Zn_4Im_4 squares are retained intact within the β-phase, and are all orientated in the same direction with respect to the crystallographic axes (Figure 4d).

The cooperative nature of the bond rearrangement can be deduced from the fact that the α→β transition is a single-crystal-to-single-crystal (SCSC) process. If bond breakage and reformation were to occur in discrete stages the formation of crystalline

Table 3. Selected Bond Lengths (Å) and Angles (deg) for the ZnIm β-Phase[a]

bond length		bond angle		bond length		bond angle	
		N1A−Zn1A−N3A	110.2(3)			N2A−Zn2A−N4A^{ii}	105.1(2)
Zn1A−N1A	2.008(6)	N1A−Zn1A−N5A	108.0(3)	Zn2A−N2A	2.008(6)	N2A−Zn2A−N6A	116.3(3)
Zn1A−N3A	1.983(6)	N1A−Zn1A−N7A	113.2(3)	Zn2A−N4A^{ii}	1.983(6)	N2A−Zn2A−N8A	108.2(2)
Zn1A−N5A	1.984(7)	N3A−Zn1A−N5A	114.0(3)	Zn2A−N6A	2.004(6)	N4A^{ii}−Zn2A−N6A	108.3(3)
Zn1A−N7A	1.979(6)	N3A−Zn1A−N7A	102.9(2)	Zn2A−N8A	1.988(6)	N4A^{ii}−Zn2A−N8A	110.8(2)
		N5A−Zn1A−N7A	108.5(3)			N6A−Zn2A−N8A	108.0(3)
		N1B−Zn1B−N3B	112.8(3)			N2B−Zn2B−N4B	102.9(3)
Zn1B−N1B	1.981(6)	N1B−Zn1B−N5B	104.5(3)	Zn2B−N2B	2.007(6)	N2B−Zn2B−N6B	110.3(3)
Zn1B−N3B	1.975(5)	N1B−Zn1B−N7B^{i}	109.9(3)	Zn2B−N4B	1.984(5)	N2B−Zn2B−N8B^{iii}	105.1(3)
Zn1B−N5B	2.019(6)	N3B−Zn1B−N5B	103.8(3)	Zn2B−N6B	1.971(6)	N4B−Zn2B−N6B	104.6(3)
Zn1B−N7B^{i}	1.980(6)	N3B−Zn1B−N7B^{i}	109.7(2)	Zn2B−N8B^{iii}	1.966(6)	N4B−Zn2B−N8B^{iii}	117.1(3)
		N5B−Zn1B−N7B^{i}	116.0(3)			N6B−Zn2B−N8B^{iii}	116.0(3)

[a] For atom labelling scheme see Figure S2 (Supporting Information). Symmetry codes: (i) $-0.5 + y, -x, 0.75 + z$; (ii) $-x, 1 - y, z$; (iii) $y, 0.5 - x, -0.75 + z$.

domains large enough to permit diffraction would be prohibited. As the β-phase crystal is a merohedral twin with four domains, we can also conclude that the transformation is initiated at discrete locations within the crystal, rather than proceeding via growth of a single β-phase domain. However, although we are able to derive a physical mechanism for the cooperative bond rearrangement by comparison of the crystal structures of the α and β phases (Figure 4b), we are not able to obtain details relating to the chemical mechanism i.e. the formation and longevity of any intermediate states involving five- or three-coordinate Zn^{2+} cations. It should also be noted that prior to the phase transition there are no statistically significant changes in the Zn−N bond lengths and N−Zn−N angles with increasing pressure (Table 2, Supporting Information Figures S3−S6). It is worth noting that the cooperative bond rearrangement mechanism by which the ZnIm phase transition proceeds is in stark contrast to the pressure-induced displacive phase transitions commonly observed in zeolitic materials.[24] The reasons for this disparity are presently unknown, and further HP-XRD experiments of MOF materials are required to clarify this matter.

During the phase change the tetragonal crystal system is retained; however, there is a 3.2% decrease in the length of the *a* axis and a 4.5% increase in the length of the *c* axis. This corresponds to a decrease in the unit cell volume of 2.1%. The origin of these changes in unit cell parameters can be explained in terms of the mechanism shown in Figure 4. The cooperative bond rearrangement occurs principally within the *ab* plane. For the reformation of the imidazolate bridge it is necessary for the Zn^{2+} that are to be linked to move closer together (Figure 4b); therefore, the distance between these two cations reduces from the nonbridged distance of 7.1072(5) Å in the α-phase, to a bridged distance of 5.934(1) Å in the β-phase. Consequently, there is an overall contraction in the *ab* plane and shortening of unit cell *a* axis. Conversely, along the [0 0 1] direction there is a lengthening of the distance between the nonbridged Zn^{2+} ions from 6.9978(4) to 7.556(1)/8.992(1) Å, and a corresponding increase in the length of the crystallographic *c* axis is observed.

Conclusion

In this contribution we report the high-pressure single-crystal X-ray diffraction analysis of a MOF. The infinite three-dimensional zinc-imidazolate complex that is central to this study undergoes a phase transition within the moderate pressure range of 0.543(5)−0.847(5) GPa. This pressure-induced conversion proceeds via an intricate cooperative bond rearrangement mechanism and results in the formation of a new phase with an unique architecture that, to the best of our knowledge, has not been prepared by conventional synthetic methods. Indeed, it is possible that the experimental apparatus detailed herein may allow for the preparation of new structural phases that may not be accessible by any other means.

This study, the first of its kind, demonstrates that high-pressure diffraction techniques can provide fundamental information pertaining to the structural evolution of hybrid MOFs in response to pressure. Such knowledge is pertinent to development of this class of materials for practical applications. Our future research objective is to expand this investigation to encompass other MOFs that exhibit a diverse range of chemical and topological properties so that we may obtain a deeper appreciation for the factors that influence their relative stabilities.

Acknowledgment. E.C.S. thanks Dr. Carla Slebodnick, Dr. Jing Zhao, and Miss Liangming Hu for their valuable advice and practical assistance. Funding from the U.S. Department of Energy, Office of Basic Energy Sciences (Grant No. DE FG03 01ER15237) and from the NSF (Grant No. EAR-0738692) is also gratefully acknowledged.

Supporting Information Available: Diagrams of the asymmetric units for both the α and β phases, bond length/angle vs pressure plots, and crystallographic data in CIF format for all structures discussed herein. This material is available free of charge via the Internet at http://pubs.acs.org.

JA808531M

(18) Von, R.; Lehnert, F.; Steel, Z. *Anorg. Allg. Chem.* **1980**, *464*, 187.
(19) O'Keeffe, M.; Eddaoudi, M.; Li, H.; Reineke, T.; Yaghi, O. M. *J. Solid State Chem.* **2000**, *152*, 3.
(20) PLATON Spek, A. L. J. Appl. Crystallogr. *36*, 7, 2003.
(21) Angel, R. J. *High-Temperature and High-Pressure Crystal Chemistry*; Hazen, R. M., Downs, R. T., Eds.; Mineralogical Society of America: Washington, DC, 2000; Vol. 41, pp 35−59.
(22) Angel, R. J. *High-Pressure Crystallography, NATO Science Series II*; Katrusiak, A., McMillan, P., Eds.; Kluwer Academic Publishers: Dordrecht; Boston, 2004; Vol. 140, pp 21−36.
(23) Boldyreva, E. V. *Acta Crystallogr.* **2008**, *A64*, 218.
(24) Gatta, G. D.; Kristallogr, Z. **2008**, *223*, 160.
(25) Moggash, S. A.; Allan, D. R.; Parsons, S.; Sawyer, L.; Warren, J. E. *J. Synchrotron Rad.* **2005**, *12*, 598.
(26) Zerilli, F. J.; Kuklja, M. M. *J. Phys. Chem. A* **2007**, *111*, 1721.
(27) Peiris, S. M.; Wong, C. P.; Zerilli, F. J. *J. Chem. Phys.* **2004**, *120*, 8060.
(28) Slebodnick, C.; Zhao, J.; Angel, R.; Hanson, B. E.; Song, Y.; Liu, Z.; Hemley, R. J. *Inorg. Chem.* **2004**, *43*, 5245.
(29) Dinnebier, R. E.; van Smaalen, S.; Olbrich, F.; Carlson, S. *Inorg. Chem.* **2005**, *44*, 964.